



**ISSN: 2454-9940**



**INTERNATIONAL JOURNAL OF APPLIED  
SCIENCE ENGINEERING AND MANAGEMENT**

**E-Mail :**  
**editor.ijasem@gmail.com**  
**editor@ijasem.org**

**www.ijasem.org**

# A UNIFIED POWER FLOW CONTROLLER USING A POWER ELECTRONICS INTEGRATED TRANSFORMER AND FUZZY CONTROLLER

<sup>1</sup>DR. S. VIJAYA MADHAVI, <sup>2</sup>ANKU KUMARI, <sup>3</sup>M. AMEENA, <sup>4</sup>B. SINDHU

## Article Info

Received: 29-01-2023

Revised: 20 -02-2023

Accepted: 2-03-2023

## Abstract:

This paper presents a Unified Power Flow Controller (UPFC) application of the Custom Power Active Transformer (CPAT); a power electronics integrated transformer which provides services to the grid through its auxiliary windings. The CPAT structure integrates three single-phase transformers into one shunt-series combining transformer. This integration empowers a sub-station with the capability of dynamically regulating the terminal voltage and current of a transformer through isolated power electronics converters. This paper investigates the CPAT's capability to provide UPFC services which includes power flow control, reactive power compensation, voltage regulation and harmonics elimination. Simulations of the CPAT-UPFC with a stiff grid and a 5-bus power system demonstrates its functionality as an inter-bus coupling transformer that provides the required grid services. Moreover, the impact of the CPAT-UPFC during load perturbations on the power system is investigated to further validate its transient and steady-state response. Furthermore, an experimental prototype reveals the operation of the three-phase CPAT-UPFC confirming its stable operation according to the theoretical expectations.

## 1. Set the Scene

Focus on renewable energy sources is growing as a result of the global economy's heavy reliance on fossil fuels and environmental concerns. Wind power is the most rapidly expanding renewable energy source in this context of increasing energy market diversity [1].

For a long time, the most common kind of wind turbine was one with a simple control system designed to save operating expenses and upkeep [1]. Electronic

converters and mechanical actuators have become more popular as a result of the growing size of turbines and the rising penetration of wind energy into the utility networks of leading nations. These active devices provide additional design flexibility that permits active regulation of the collected energy. As an interface to the power grid, static converters allow for variable-speed operation up to the rated speed.

<sup>1</sup>ASSOCIATE PROFESSOR &HOD, <sup>2,3,&4</sup> UG SCHOLAR

DEPARTMENT OF EEE,

MALLA REDDY ENGINEERING COLLEGE FOR WOMEN, HYDERABAD

Variable speed control seems to be a viable alternative for improving the functioning of wind turbines in the face of environmental disturbances including random wind variations, wind shear, and tower shadows [2]. From a control system perspective, wind energy conversion systems provide unique difficulties. Due to their nonlinear nature and susceptibility to significant cyclic disturbances, wind turbines may experience excitation of the weakly damped vibration modes of the drive-train and tower (see [1, 3]). Because of their unique working circumstances, wind turbines are notoriously difficult to model mathematically so that their dynamic behavior may be precisely described. The present trend toward bigger and more adaptable wind turbines makes this work much more complex. Robust control techniques that can provide stability and certain performance aspects despite model uncertainties are needed to offset the absence of precise models. Turbines with variable speed and pitch increase the complexity of the control difficulties, as shown in [4-6]. Multiple controls are required for optimal performance of this kind of turbine (see to [7, 8] for details).

In this study, we suggest a novel approach to controlling horizontal-axis wind turbines (HAWTs) that may vary both in speed and pitch. This regulation is accomplished by a proportional integral (PI) controller for the blade pitch angle and a nonlinear dynamic chattering torque control approach. With the help of this novel control mechanism, the amount of electricity produced by a wind turbine may be rapidly changed between several preset levels. This suggests that WT power generation may be adjusted up or down

depending on network demand for electricity. All other state variables, such as the rotational speeds of the turbines and generators, as well as the smooth and appropriate development of the control variables, guarantee this electrical power tracking.

This paper will proceed as described below. Wind turbine modeling is covered in Section 2. In Section 3, we get a quick rundown of the FAST code [9], a wind turbine simulator developed by the National Renewable Energy Laboratory. Following this, Section 4 details the pitch and torque controls. Section 5 concludes by validating the suggested controllers using the FAST aero elastic wind turbine simulator and comparing their performance to that of controllers proposed in [10, 11] to emphasize the enhancements of the offered technology.

### **Modeling Systems**

The wind generator has a rotor, transmission, and generator. The rotor of a wind turbine captures the wind's kinetic energy and transforms it into mechanical work. The rotor was modeled using simplifications in [12-14]. With this model, we assume the following equation about the relationship between wind speed and the resulting mechanical power:

$$P_m(u) = \frac{1}{2} C_p(\lambda, \beta) \rho \pi R^2 u^3$$

Where  $\rho$  is the air density, R is the rotor radius, u is the wind speed, and  $C_p$  is the wind turbines power coefficient the ratio of the pitch angle to the tip speed is denoted by

$$\lambda = \frac{R\omega_r}{u}$$

for which  $\omega_r$  stands for rotor velocity. Therefore, the power produced is impacted by changes in wind speed or rotor speed, since they alter the tip-speed ratio, which in turn affects the power coefficient. The relationship between the power coefficient and the aerodynamic torque coefficient is as follows,

$$P_m = \omega_r T_a$$

the aerodynamic torque expression is described as

$$T_a = \frac{1}{2} C_q(\lambda, \beta) \rho \pi R^3 u^2$$

Where

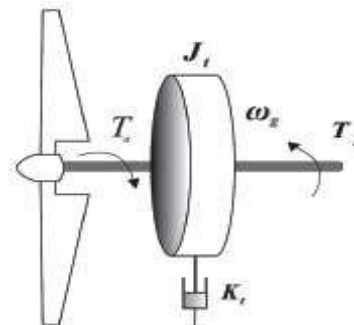
$$C_q(\lambda, \beta) = \frac{C_p(\lambda, \beta)}{\lambda}$$

A single-mass model of a wind turbine may be studied for a fully stiff low-speed shaft [10,15-17].

$$J_t \dot{\omega}_r = T_a - K_t \omega_r - T_g$$

where  $T_a$  is the aerodynamic torque (Nm),  $T_g$  is the generator torque (Nm),  $J_t$  is the turbine's total inertia (kg m<sup>2</sup>), and  $K_t$  is the turbine's total external damping (Nm rad<sup>-1</sup> s). Figure 1 depicts the overall plan of the one-mass model.

*Wind turbine mass model shown in Figure 1.*



### 3. The Short Synopsis of a Simulator (FAST)

Two- and three-blade HAWTs' extreme and fatigue loads may be predicted with the use of the FAST programme [9], a robust aeroelastic simulator. Due to Germanischer Lloyd WindEnergie's positive evaluation of this simulator back in 2005, it was selected for validation [18]. This simulator is used to calculate loads for onshore wind turbines throughout the design and certification processes. To make it easier for users to build complex turbine controls in Simulink R, a block

diagram interface was created in MATLAB R. The FAST motion equations (in an S-function) are integrated into a Simulink model by connecting the FAST subroutines with a Matlab standard gateway subroutine. This provides a great deal of leeway for how simulations of wind turbine controls are implemented. The full nonlinear aeroelastic wind turbine equations of motion are available in FAST, and may be used in the Simulink environment to develop and simulate control modules for the generator torque, nacelle yaw, and pitch. Blocks that integrate accelerations in different degrees of freedom to get velocities and displacements are included in the wind turbine block, along with an S-function block containing the FAST motion equations. That's why we use one of Simulink's solvers to work out the equations of motion, which we write in the form of a FAST S-function.

## **FUZZY CONTROLLER**

"Fuzzy control" and "Fuzzy Control" redirect here. For the rock band, see Fuzzy Control (band) A fuzzy control system is a control system based on fuzzy logic—a mathematical system that analyzes analog input values in terms of logical variables that take on continuous values between 0 and 1, in contrast to classical or digital logic, which operates on discrete values of

either 1 or 0 (true or false, respectively) Fuzzy logic is widely used in machine control. The term "fuzzy" refers to the fact that the logic involved can deal with concepts that cannot be expressed as the "true" or "false" but rather as "partially true". Although alternative approaches such as genetic algorithms and neural networks can perform just as well as fuzzy logic in many cases, fuzzy logic has the advantage that the solution to the problem can be cast in terms that human operators can understand, so that their experience can be used in the design of the controller. This makes it easier to mechanize tasks that are already successfully performed by humans History and applications

Fuzzy logic was proposed by Lotfi A. Zadeh of the University of California at Berkeley in a 1965 paper.[3] He elaborated on his ideas in a 1973 paper that introduced the concept of "linguistic variables", which in this article equates to a variable defined as a fuzzy set. Other research followed, with the first industrial application, a cement kiln built in Denmark, coming on line in 1975.

Fuzzy systems were initially implemented in Japan.

Interest in fuzzy systems was sparked by Seiji Yasunobu and Soji Miyamoto of Hitachi, who in 1985 provided simulations that demonstrated the feasibility of fuzzy control systems for the Sendai Subway. Their ideas were adopted, and fuzzy systems were used to control accelerating, braking, and stopping when the Namboku Line opened in 1987.

In 1987, Takeshi Yamakawa demonstrated the use of fuzzy control, through a set of simple dedicated fuzzy logic chips, in an "inverted pendulum" experiment. This is a classic control problem, in which a vehicle tries to keep a pole mounted on its top by a hinge upright by moving back and forth. Yamakawa subsequently made the demonstration more sophisticated by mounting a wine glass containing water and even a live mouse to the top of the pendulum: the system maintained stability in both cases. Yamakawa eventually went on to organize his own fuzzy-systems research lab to help exploit his patents in the field.

Japanese engineers subsequently developed a wide range of fuzzy systems for both industrial and consumer applications. In 1988 Japan established the Laboratory for International Fuzzy Engineering (LIFE), a cooperative arrangement between 48 companies to pursue fuzzy research. The automotive

company Volkswagen was the only foreign corporate member of LIFE, dispatching a researcher for a duration of three years.

Japanese consumer goods often incorporate fuzzy systems. Matsushita vacuum cleaners use microcontrollers running fuzzy algorithms to interrogate dust sensors and adjust suction power accordingly. Hitachi washing machines use fuzzy controllers to load-weight, fabric-mix, and dirt sensors and automatically set the wash cycle for the best use of power, water, and detergent.

Canon developed an autofocus camera that uses a charge-coupled device (CCD) to measure the clarity of the image in six regions of its field of view and use the information provided to determine if the image is in focus. It also tracks the rate of change of lens movement during focusing, and controls its speed to prevent overshoot. The camera's fuzzy control system uses 12 inputs: 6 to obtain the current clarity data provided by the CCD and 6 to measure the rate of change of lens movement. The output is the position of the lens. The fuzzy control system uses 13 rules and requires 1.1 kilobytes of memory.

An industrial air conditioner designed by Mitsubishi uses 25 heating rules and 25

cooling rules. A temperature sensor provides input, with control outputs fed to an inverter, a compressor valve, and a fan motor. Compared to the previous design, the fuzzy controller heats and cools five times faster, reduces power consumption by 24%, increases temperature stability by a factor of two, and uses fewer sensors.

Other applications investigated or implemented include: character and handwriting recognition; optical fuzzy systems; robots, including one for making Japanese flower arrangements; voice-controlled robot helicopters (hovering is a "balancing act" rather similar to the inverted pendulum problem); rehabilitation robotics to provide patient-specific solutions (e.g. to control heart rate and blood pressure [4]); control of flow of powders in film manufacture; elevator systems; and so on.

Work on fuzzy systems is also proceeding in North America and Europe, although on a less extensive scale than in Japan.

The US Environmental Protection Agency has investigated fuzzy control for energy-efficient motors, and NASA has studied fuzzy control for automated space docking: simulations show that a fuzzy control system can greatly reduce fuel consumption.

Firms such as Boeing, General Motors, Allen-Bradley, Chrysler, Eaton, and Whirlpool have worked on fuzzy logic for use in low-power refrigerators, improved automotive transmissions, and energy-efficient electric motors.

In 1995 Maytag introduced an "intelligent" dishwasher based on a fuzzy controller and a "one-stop sensing module" that combines a thermistor, for temperature measurement; a conductivity sensor, to measure detergent level from the ions present in the wash; a turbidity sensor that measures scattered and transmitted light to measure the soiling of the wash; and a magnetostrictive sensor to read spin rate. The system determines the optimum wash cycle for any load to obtain the best results with the least amount of energy, detergent, and water. It even adjusts for dried-on foods by tracking the last time the door was opened, and estimates the number of dishes by the number of times the door was opened.

In 2017 Xiera Technologies Inc. developed the first auto-tuner for the fuzzy logic controller's knowledge base known as eX. This technology was tested by Mohawk College and was able to solve non-linear 2x2 and 3x3 multi-input multi-output problems.[5]

Research and development is also continuing on fuzzy applications in software, as opposed to firmware, design, including fuzzy expert systems and integration of fuzzy logic with neural-network and so-called adaptive "genetic" software systems, with the ultimate goal of building "self-learning" fuzzy-control systems.[6] These systems can be employed to control complex, nonlinear dynamic plants,[7] for example, human body.[4][6][8]

#### Fuzzy sets

See also: fuzzy set

The input variables in a fuzzy control system are in general mapped by sets of membership functions similar to this, known as "fuzzy sets". The process of converting a crisp input value to a fuzzy value is called "fuzzification". The fuzzy logic based approach had been considered by designing two fuzzy systems, one for error heading angle and the other for velocity control.[9]

A control system may also have various types of switch, or "ON-OFF", inputs along with its analog inputs, and such switch inputs of course will always have a truth value equal to either 1 or 0, but the

scheme can deal with them as simplified fuzzy functions that happen to be either one value or another.

Given "mappings" of input variables into membership functions and truth values, the microcontroller then makes decisions for what action to take, based on a set of "rules", each of the form:

IF brake temperature IS warm AND speed IS not very fast

THEN brake pressure IS slightly decreased.

In this example, the two input variables are "brake temperature" and "speed" that have values defined as fuzzy sets. The output variable, "brake pressure" is also defined by a fuzzy set that can have values like "static" or "slightly increased" or "slightly decreased" etc.

#### Fuzzy control in detail

Fuzzy controllers are very simple conceptually. They consist of an input stage, a processing stage, and an output stage. The input stage maps sensor or other inputs, such as switches, thumbwheels, and so on, to the appropriate membership



functions and truth values. The processing stage invokes each appropriate rule and generates a result for each, then combines the results of the rules. Finally, the output stage converts the combined result back into a specific control output value.

The most common shape of membership functions is triangular, although trapezoidal and bell curves are also used, but the shape is generally less important than the number of curves and their placement. From three to seven curves are generally appropriate to cover the required range of an input value, or the "universe of discourse" in fuzzy jargon.

As discussed earlier, the processing stage is based on a collection of logic rules in the form of IF-THEN statements, where the IF part is called the "antecedent" and the THEN part is called the "consequent". Typical fuzzy control systems have dozens of rules.

Consider a rule for a thermostat:

IF (temperature is "cold") THEN turn  
(heater is "high")

This rule uses the truth value of the "temperature" input, which is some truth value of "cold", to generate a result in the fuzzy set for the "heater" output, which is some value of "high". This result is used with the results of other rules to finally generate the crisp composite output. Obviously, the greater the truth value of "cold", the higher the truth value of "high", though this does not necessarily mean that the output itself will be set to "high" since this is only one rule among many. In some cases, the membership functions can be modified by "hedges" that are equivalent to adverbs. Common hedges include "about", "near", "close to", "approximately", "very", "slightly", "too", "extremely", and "somewhat". These operations may have precise definitions, though the definitions can vary considerably between different implementations. "Very", for one example, squares membership functions; since the membership values are always less than 1, this narrows the membership function. "Extremely" cubes the values to give greater narrowing, while "somewhat" broadens the function by taking the square root.

In practice, the fuzzy rule sets usually have several antecedents that are combined using fuzzy operators, such as AND, OR,

and NOT, though again the definitions tend to vary: AND, in one popular definition, simply uses the minimum weight of all the antecedents, while OR uses the maximum value. There is also a NOT operator that subtracts a membership function from 1 to give the "complementary" function. There are several ways to define the result of a rule, but one of the most common and simplest is the "max-min" inference method, in which the output membership function is given the truth value generated by the premise

Rules can be solved in parallel in hardware, or sequentially in software. The results of all the rules that have fired are "defuzzified" to a crisp value by one of several methods. There are dozens, in theory, each with various advantages or drawbacks.

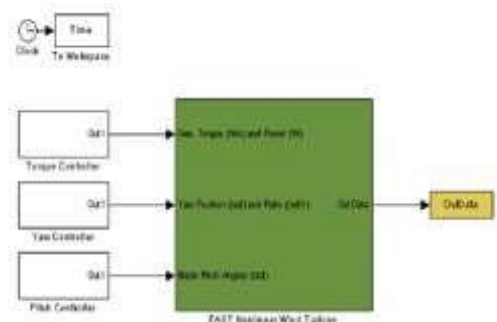
The "centroid" method is very popular, in which the "center of mass" of the result provides the crisp value. Another approach is the "height" method, which takes the value of the biggest contributor. The centroid method favors the rule with the output of greatest area, while the height method obviously favors the rule with the greatest output value.

The diagram below demonstrates max-min inferencing and centroid defuzzification for a system with input variables "x", "y", and "z" and an output variable "n". Note that "mu" is standard fuzzy-logic nomenclature for "truth value":

#### 4 Methods of Regulation

Thanks to the MATLAB R interface we created between FAST and Simulink, the suggested torque and pitch controls may be easily implemented in block diagram form in Simulink R. The FAST simulink open-loop model is shown in Figure 2.

*Open-loop Simulink model shown in Figure 2.*



In the following paragraphs, we will discuss the suggested designs for a nonlinear dynamic torque controller and a linear pitch controller.

#### Torque Control Unit (TCU) 4.1

The definition of the electrical power-tracking mistake is

$$e = P_e - P_{ref} \quad (1)$$

where  $P_e$  is the power output of an electrical source and  $P_{ref}$  is the standard power. To this flow, we apply a first-order dynamic,

$$\dot{e} = -ae - K_\alpha \text{sgn}(e) \quad a, K_\alpha > 0 \quad (2)$$

Now think about how [10,15,17,19] describes the electrical current.

$$P_e = \tau_c \omega_g \quad (3)$$

where  $\omega_g$  is the generator speed and  $\tau_c$  is the torque control. When we assume that  $P_{ref}$  is a constant function and plug its values into Equations (1) and (3), we get

$$\tau_c \dot{\omega}_g + \tau_c \omega_g = -a(\tau_c \omega_g - P_{ref}) - K_\alpha \text{sgn}(\tau_c \omega_g - P_{ref})$$

which, can also be written as

$$\dot{\tau}_c = \frac{-1}{\omega_g} [\tau_c (\omega_g + \dot{\omega}_g) - aP_{ref} + K_\alpha \text{sgn}(\tau_c \omega_g - P_{ref})] \quad (4)$$

4.1 Theorem [20] The suggested controller 4 guarantees stability over limited intervals of time. Also, by appropriately specifying the values of the parameters  $a$  and  $K_\alpha$ , the settling time may be selected.

**Proof The Lyapunov function is introduced here.**

$$V = \frac{1}{2} e^2 \quad (5)$$

The time derivative of the system's trajectory then gives rise to

$$\dot{V} = e\dot{e} = e(-ae - K_\alpha \text{sgn}(e)) = -ae^2 - K_\alpha |e| < 0 \quad (6)$$

The time derivative of the Lyapunov-candidate-function is worldwide negative definite, and because  $V$  is globally positive definite and radially unbounded, this proves that the equilibrium is globally asymptotically stable. In addition, proof of stability in limited time is possible. The equivalent form of (6) is

$$\dot{V} \leq -K_\alpha |e| = -K_\alpha \sqrt{2} \sqrt{V}$$

Thus,

$$\dot{V} + K_\alpha \sqrt{2} \sqrt{V}$$

is negative semidefinite, thus we can use Theorem 1 from [20] to verify that our starting point is a stable equilibrium that holds for finitely long periods of time. Additionally, the settling time function is defined as in [20].

$$t_s \leq \frac{1}{K_\alpha \sqrt{2}} (V)^{1/2}$$

and using Equation (5) leads to

$$t_s \leq \frac{e}{K_\alpha} \quad (7)$$

For  $K_\alpha = 0$ , we have an exponentially stable (but not finite-time) controller.

$$\dot{e} = -ae \quad (8)$$

Then, we pick a substantially shorter settling time for the finite time stable strategy by computing an estimated settling time (for practical reasons) for the exponentially stable controller. We do this by contrasting the simplest resistor-capacitor (RC) circuit with the exponentially stable error dynamic, given by Equation (8). One resistor (R) and one capacitor (C) are connected in series to form this circuit. A charged capacitor and a resistor are all that's needed to complete a circuit, and the capacitor will release its charge via the resistor. Kirchhoff's current law may be used to calculate the time-varying voltage,  $v$ , across the capacitor. As a consequence, we have the linear differential equation given by

$$C\dot{v} + \frac{v}{R} = 0 \quad (9)$$

This first-order differential equation has a well-known exponential decay solution.

$$v(t) = v_0 e^{-\frac{t}{RC}}$$

where  $v_0$  is the voltage across the capacitor at instant  $t = 0$ . The time constant,  $\tau = RC$ , is defined as the amount of time needed for the voltage to drop to  $v_0 = e$ . According to [21], after around  $5\tau$  s, the capacitor is deemed to have completely depleted (0.7%).

Equation (9) for the RC circuit's ODE is equivalent to Equation (8) for an exponentially stable error dynamic, hence we get  $a = 1$  RC for any value of  $a$ . It will take  $5\tau$  to get the target number with an error of 0.7% if the error dynamic is exponentially steady. Using Equation (7), we may choose parameters to get the required value in  $0.2(5\tau)$  s, as our suggested controller is finite-time stable. Accordingly, at times around  $t = 0$ , the error is constrained by  $|e| \leq 1.5 \times 10^6$  (the rated power of the wind turbine).

$$t_s \leq \frac{1.5 \times 10^6}{K_a} < 0.2(5\tau) = 0.2(5\frac{1}{a})$$

For  $a = 1$ , the estimated settling time is less than one second,

$$t_s \leq \frac{1.5 \times 10^6}{K_a} < 1 \quad (10)$$

and, by rearranging terms, the value of  $K_a$  should be,

$$K_a > 1.5 \times 10^6$$

Take into account the  $\omega$  dependence of Equation (4). Wind turbine characteristics such as total inertia, total external damping, aerodynamic torque, generator torque at rotor side, and gearbox ratio are needed to calculate this derivative using the one-mass model of a wind turbine provided in Section 2. The estimator

presented in [22] (transfer function in the Laplace domain) is another option for calculating this derivative.

$$\frac{s}{0.1s + 1} \quad (11)$$

Equation (11) takes  $\dot{g}$  as input and estimates  $\ddot{g}$  as output.

Neither the whole external damping nor the total inertia of the turbine is needed for the suggested simple nonlinear torque control Equation (4). The WT's generator speed and electrical output are all that's needed to operate this control. Thus, to approximate  $\ddot{g}$  using our suggested controller and Equation (11), only a small number of WT parameters are needed. When compared to this, most torque controllers in the literature [10,15-17] need a large number of WT parameters, limiting the controller's usefulness when some but not all of these data are unavailable.

#### 4.2 Pitch Regulator

The rotor speed tracking error is supplemented by a pitch proportional integral (PI) controller to help the torque controller manage the wind turbine's electrical power production while avoiding excessive loads and keeping the rotor speed within safe parameters.

$$\beta = K_p(\omega_r - \omega_n) + K_i \int_0^t (\omega_r - \omega_n) dt, \quad K_p > 0, K_i > 0$$

where  $r$  is the rated electrical power output of the wind turbine and  $n$  is the nominal rotor speed. The following phrase describes the final suggested controller, which turns off the proportional term when  $r \leq n$ .

$$\beta = \frac{1}{2} K_p (\omega_r - \omega_n) [1 + \text{sign}(\omega_r - \omega_n)] + K_i \int_0^t (\omega_r - \omega_n) dt, \quad K_p > 0, K_i > 0$$

### Five, The Simulation Outcomes

The NREL WP 1.5 MW wind turbine was used for numerical validations using FAST on Matlab-Simulink. Table 1 provides a brief overview of the various wind turbine features.

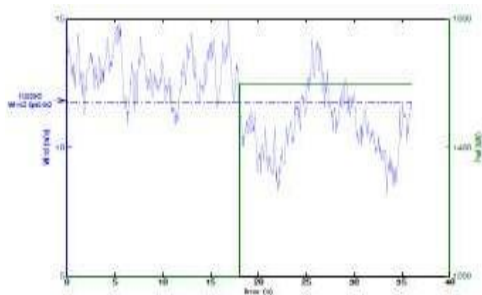
Wind turbine features are shown in Table 1.

Number of blades	3
Height of tower	82.39 m
Rotor diameter	70 m
Rated power	1.5 MW
Gearbox ratio	87.965
Nominal rotor speed ( $\omega_n$ )	20 rpm

Figure 3 depicts the simulated wind influx. WT electrical power is subject to a changeable reference set point. If the wind park management needs a certain amount of electricity, he or she must allocate this demand among the park's turbines and set a unique reference for each one. The

simulated NREL WP 1.5-MW wind turbine experiences wind speeds in excess of its rated power operating parameters during this wind influx. The mean wind speed profile in Figure 3 corresponds with the rated wind speed of the wind turbine, which is 11:8 m/s. The reference power is also shown (right y-axes) in Figure 3.

Diagram 3. Average wind speed of 11:8 m/s, which is the WT's recommended maximum (left y-axes). The y-axis on the right represents power.



### Torque and Pitch Regulation 5.1

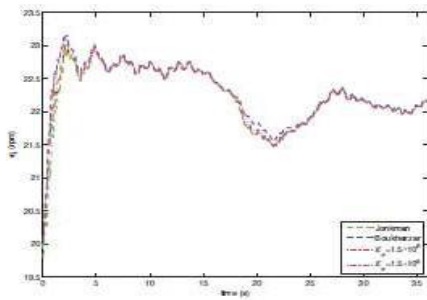
Torque and pitch control outputs from the FAST simulator are calculated using  $a = 1$ ,  $K_p = 1$ ,  $K_i = 1$ , and two values for  $K_{\omega}$  (different settling times):  $K_{\omega} = 1:5\ 106$  and  $K_{\omega} = 1:5\ 105$ . Control schemes presented in [10] (Bukhezzar's controller) and [11] (Jonkman's controller) are evaluated and contrasted with these findings.

Figure 4 demonstrates that owing to the pitch control action, the rotor speed is very

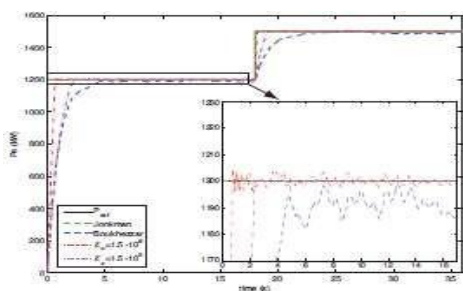
close to the nominal value (20 rpm) for all tested controllers.

Figure 5 shows that when the reference electrical power is altered, the Boukhezzar controller converges exponentially to the intended value in about 5 seconds. Torque controllers like the Jonkman achieve almost flawless power regulation, but as we'll see, they also produce loads that far exceed their intended capacity. Our suggested controller exhibits characteristics that fall somewhere in the middle of those of Jonkman's and Boukhezzar's. When the parameter  $K_{\omega} = 1:5106$ , the electrical power tracks the reference despite changes in the wind speed, with a settling period of one second [see Equation (10)]. Similar results are achieved, but with a lengthier settling period, when parameter  $K_{\omega} = 1:5\ 105$  is utilized. By adjusting the settling time, our controller may be made to more closely resemble the controllers proposed by Jonkman and Boukhezzar. Our controller has limited convergence, thus it takes longer time than the Boukhezzar's controller to get to the reference power. Figure 5 shows this pattern in further detail.

**Rotor velocity, seen in Fig.**

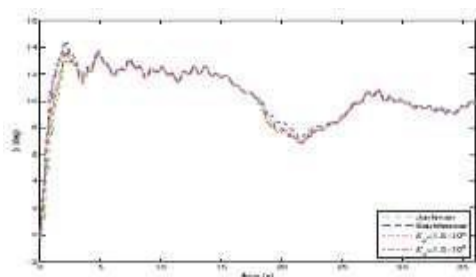


**Figure 5. Power output.**



Depending on the turbine's power, the maximum pitch rate may be anywhere from 8 /s for 5 MW turbines to 18 /s for 600 kW research turbines [23]. As can be seen in Figure 6, all of the evaluated controllers keep the blade pitch angle from deviating more than 10 degrees per second within the permitted variation region.

**Figure 6. Pitch control.**



From Figure 7, the torque action of the proposed controller is smooth and achieves reasonable values,

controls like those achieved by Jonkman and Boukhezzar. Depending on the load, the generator may not be able to provide the required amount of electro-mechanical torque. Saturating the torque control at more than 10% over the rated value (about 7:7 kNm) might cause the motor to overheat and fail (see [11] for further information). None of the controllers undertest go as high as the value shown in Figure 7.

It is also crucial to consider how loads influence the control behavior. Figure 8 depicts the tower bottom side-to-side moment, Figure 9 the torsion of the drive shaft, Figure 10 the roll moment of the tower top/yaw bearing, and Figure 11 the side-to-side shear force of the tower top/yaw bearing. In all but one scenario, the Jonkman controller reaches loads very close to the design load while maintaining virtually flawless power regulation. Boukhezzar's controller, on the other hand, makes advantage of intermediate loads yet demonstrates subpar performance for power regulation. Finally, our controller strikes the optimal balance between load capacity and responsiveness to variations in required power.

**Figure 7. Torque control.**

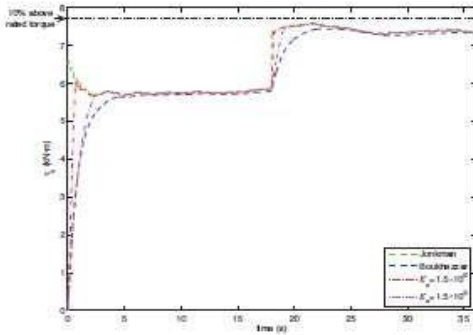


**Figure 8. Tower bottom side-to-side moment.**

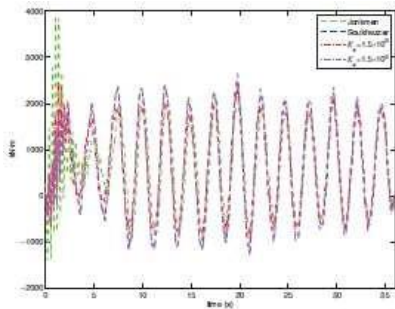


**Figure 9. Drive shaft torsion.**

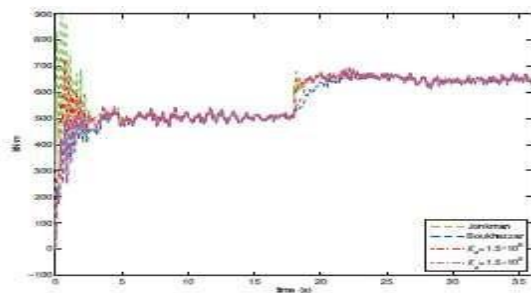


**Figure 10. Tower top/yaw bearing roll moment.**

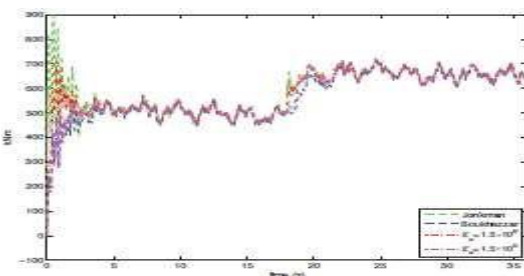


**Figure 11. Tower top/yaw bearing side-to-side shear force.**

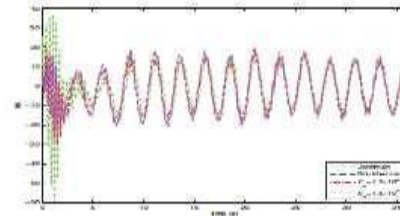
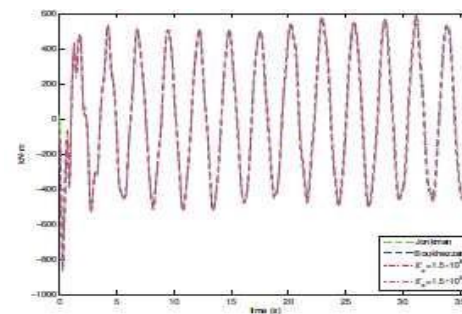


Figure 12 depicts another crucial load, the bending moment at the blade's edge, which yields the same results for all the tested controllers.

**Figure 12. Blade edge-wise bending moment.**



Finally, a fatigue study was conducted using the MatLab postprocessor MCrunch [24] for wind turbine data analysis. Damage equivalent loads are shown in Table 2, and the cumulative rainflowcycles of relevant loads from simulations up to 600 s are displayed in Figure 13; the reference power varies between 1200 and 1500 kW every 18 s. WindPACT turbine documentation [25] is mined for the fatigue design SN slopes. A notable fatigue variance is seen in the first



cumulative cycles per second for loads such as drive shaft torsion and tower top/yaw bearing roll moment when using Jonkman's controller. This is consistent with what was shown in the previous section, when it was shown that the controller was capable of loading approaching but not quite reaching the design load.

List of equal loads to cause damage, table 2.

	Units	SN Slope	$K_a = 1.5 \times 10^5$	$K_a = 1.5 \times 10^6$	Boukhezzar	Jonkm
Tower bottom						
side-to-side	(kN-m)	3	$1.255 \times 10^5$	$1.195 \times 10^5$	$1.174 \times 10^5$	$1.418 \times 10^5$
Drive shaft	(kN-m)	6.5	$1.086 \times 10^2$	$1.459 \times 10^2$	$1.295 \times 10^2$	$3.080 \times 10^2$
Tower top/yaw bearing roll	(kN-m)	3	$7.699 \times 10^1$	$8.144 \times 10^1$	$7.338 \times 10^1$	$1.080 \times 10^2$
Tower top/yaw side-to-side	(kN)	3	$1.555 \times 10^3$	$1.501 \times 10^3$	$1.473 \times 10^3$	$1.444 \times 10^3$
Blade edge-wise bending	(kN-m)	8	$1.237 \times 10^5$	$9.599 \times 10^4$	$9.562 \times 10^4$	$9.595 \times 10^4$

Figure 13. Cumulative rainflow cycles.

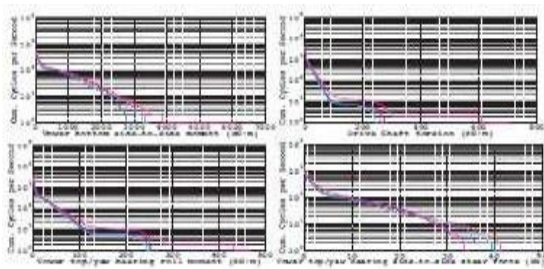


Figure 13. Cont.

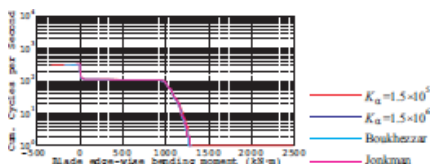
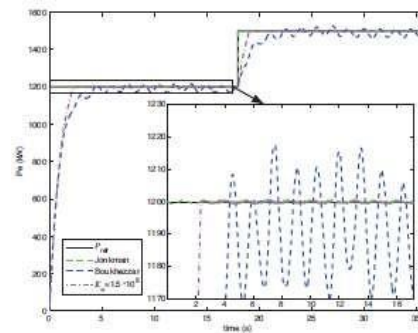


Figure 14. Power output with a periodic noise signal.

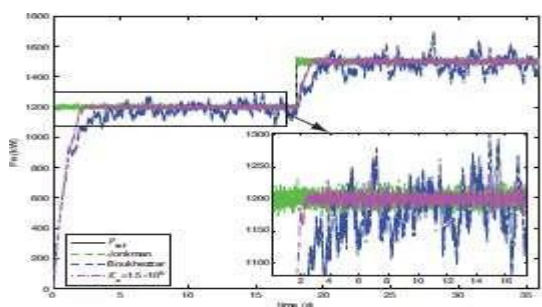


Using Intermittent Signals to Regulate Pitch and Torque

The proposed generator torque and blade pitch controls rely only on the generator speed measurement, as is common for utility-scale multi-megawatt wind turbines. To account for signal noise (which occurs in practical contexts), the conventional method of measuring a generator's output is supplemented with a sine wave with amplitude 1:1 and frequency 2:1 the nominal rotor speed. Since periodic disturbances exist in rotating mechanical systems, testing for their absence is the initial step (see [26,27] for more information). Figure 14 shows, enlarged, that compared to the other evaluated controllers, our suggested controller is more resistant to periodic noise signals. The findings show that Boukhezzar's controller is much more vulnerable to noise than the one shown in Figure 5. Although Jonkman's controller provides almost ideal power regulation, it is

impacted by noise in the input signals. Although the low-pass filter of Jonkman's controller is detailed in [11], the corner frequency of this filter is 0.25 Hz, hence the noisy signal is not filtered out in this situation. Jonkman's controller may benefit from a different kind of filter, and the same is true for Boukhezzar's controller in certain cases. Nevertheless, our controller performs well even without filters. The white noise signal is finally evaluated. Figure 15 shows a zoomed-in view of the scene, revealing that the noise has a far greater impact on Boukhezzar's controller. In this scenario, our suggested controller performs similarly to Jonkman's controller.

***White noise signal power output is shown in Figure 15.***



### Concluding Remarks

This research presents a WT controller optimized for use in high-turbulence wind environments. Strong performances in rotor speed and electrical power management are achieved with satisfactory control activity using the suggested

controller. These findings demonstrate that the suggested controller enables a range of values to be selected for the output power from the WT generator. This success implies that WT power production can be scaled up or down in response to the network's power consumption and that WTs can take part in the primary grid's frequency control, allowing for a greater percentage of wind to be incorporated into electric networks without negatively impacting the quality of the generated electric power.

Finally, we detail how the suggested controller is superior than the previously tested methods.

Finite-time stability is guaranteed by the suggested controller. Thus, the suggested controller is superior than exponentially stable controllers like [10] in that it more accurately meets the target power reference.

By appropriately specifying the values of the parameters  $a$  and  $K_$  in Equation (4), the proposed controller enables the settling time to be selected. It is possible to produce intermediate controllers with settling times between those of the Jonkman and Boukhezzar controllers by modifying our controller.

- The suggested simple nonlinear torque controller just needs the generator speed and electrical power of the WT, not the

turbine's complete external damping or inertia. Therefore, the suggested controller may be simply implemented in various WTs. Better results may be achieved using a simpler model than that used in [10].

- The suggested controller strikes a good balance between load balancing and responding to variations in the amount of electricity that is needed.

It is not necessary to use filters with the suggested controller since it is more resistant to periodic noise signals.

## REFERENCES

1. Wind Energy Handbook; Wiley: Chichester, UK, 2001. 1. Burton, T.; Sharpe, D.; Jenkins, N.; Bossanyi, E. Zinger, D. and Muljadi, E. Annualized wind energy improvement with variable speeds. 1997, Volume 33, Issues 1444–1447 of the IEEE Transactions on Industrial Applications.
2. Kusiak, A., & Zhang, Z. Data-driven control of power and vibration in wind turbines. *Energy Renewables* 2012, 43,
3. P.Hassan, H.M., A.L. Eishafei, W.A. Farag, and M.S. Saad are the four authors. Controlling the pitch of very big wind turbines using strong LMI. *Energy Renew* 2012, 44, p.
4. Individual pitch control of horizontal axis wind turbines. Sandquist, F., G. Moe, & O. Anaya-Lara. 2012, 134, DOI:10.1115/1.4005376,
5. J. Offshore Mech. Arctic Eng.-Trans. ASME. Using pitch control based on a disturbance observer, Joo, Y., and Back, J., regulate the power output of variable-speed wind turbines. *Electr. Eng. & Technol.*, 2012, 7, 273-280. H-infinity based control for load mitigation in wind turbines.
6. Diaz de Corcuera, A.; Pujana-Arrese, A.; Ezquerro, J.M.; Seguro, E.; Landaluze, J. (2012) 5(5):938-967, *Energy*. Using Multiple Models for MIMO Predictive Control of VSP Wind Turbines, by Soliman, Malik, and Westwick (2008)
7. American Control Conference Proceedings, Baltimore, Maryland, USA, 30 June-2 July 2010. NWT Design Codes (FAST)
8. Jonkman, J. The design codes and simulators are available at <http://wind.nrel.gov/designcodes/fast/>. (retrieved: March 8, 2012).
9. Boukhezzar, B.; Lupu, L.; Siguerdidjane, H.; Hand, M. Strategy for controlling wind turbines with several variables.

